NATIONAL ADVISORY COMMITTEE FOR AERONAUTICS

WARTIME REPORT

ORIGINALLY ISSUED
December 1942 as
Advance Restricted Report

THE STRENGTH AND STIFFNESS OF SHEAR WEBS WITH ROUND LIGHTENING HOLES HAVING 45° FLANGES

By Paul Kuhn

Langley Memorial Aeronautical Laboratory
Langley Field, Va.

NACA

WASHINGTON

NATIONAL ADVISORY COMMITTEE FOR AERONAUTICS

ADVANCE RESTRICTED REPORT

THE STRENGTH AND STIFFNESS OF SHEAR WEBS WITH ROUND LIGHTENING HOLES HAVING 45° FLANGES

By Paul Kuhn

SUMMARY

Tests were made of 18 shear webs with round lightening holes having 45° flanges. The purpose of the tests was to extend the range of a previous investigation to larger ratios of hole diameter to web depth and of web depth to web thickness. Simple empirical formulas are given for the strength and the stiffness of shear webs; these formulas incorporate the results of the previous investigation. Design charts are also given to facilitate the application of the results.

INTRODUCTION

As part of a general investigation on shear webs, a number of webs with flanged, round lightening holes had been tested and an empirical formula for the strength of the webs had been obtained (reference 1).[1] Although the number of specimens was fairly large, the range of some of the variables was quite limited in comparison with the range that might be possible in actual construction. In the development of the strength formula, an attempt was made to compensate for this inadequacy of the test data by considering limiting cases in order to find a formula that might give reasonable accuracy when extrapolated beyond the test range. In view of the narrow range over which the formula was actually verified, however, it was considered desirable to make at least a small number of tests of webs having larger ratios of hole diameter to web depth and of web depth to web thickness.

The Bell Aircraft Corp., which had contributed the specimens for the original investigation, cooperated by furnishing the specimens for this extension of the work.

---

[1]The data contained in this report supersede the part of reference 1 dealing with webs having lightening holes with 45° flanges.

SYMBOLS

The symbols used in the present report are contained in the following list. All lengths are expressed in inches; all stresses, in kips per square inch; and all loads, in kips.

D	clear diameter of hole
L	length of specimen
P	any load acting on shear web in jig
P_{av}	average value of collapsing load
P_s	load at which permanent set was measured
P_{all}	allowable load suggested for use in design
P_{coll}	load causing collapse of specimen
P_{cr}	load causing buckling
S	transverse shear force on web
V	volume of web material per inch run, cubic inches per inch
b	hole spacing, center-to-center
c	length of space between holes (b-D)
c'	flat portion of length c
h	depth of web (rivet line to rivet line)
L_e	effective length of solid web
t	thickness of web
η	factor for shear stiffness at any load within elastic range
η_o	factor for initial shear stiffness
τ	shear stress

L-323

τ_{cr} critical shear stress (theoretical)

τ_c shear stress causing collapse of a long plate of width c and thickness t (from curves for τ_{coll} in fig. 3)

τ_h shear stress causing collapse of a long plate of width h and thickness t (from curves for τ_{coll} in fig. 3)

$\tau_{c_{cr}}$ critical shear stress of a long plate of width c and thickness t, assuming supported edges (from curve for τ_{cr} in fig. 3)

$\tau_{h_{cr}}$ critical shear stress of a long plate of width h and thickness t, assuming supported edges (from curve for τ_{cr} in fig. 3)

τ_{coll} shear stress causing collapse of a web. With a perforated web, the stress is based on the gross section. Unless the stress in a perforated web is specifically designated experimental, the stress calculated by formula (4) is meant.

k_{av}, k_{all} correction factors

TEST PROCEDURE

Test specimens.- The important dimensions of the test specimens are given in tables 1 and 2. The material of all specimens was 24S-T aluminum alloy. The flanges around the holes were the manufacturer's standard flanges of nominally 45^o; the ratio of the clear diameter of a hole to the root diameter was about 0.9. The standard shape of specimen chosen is shown in figure 1. On some specimens, the flanges at the ends of the specimen were reinforced by riveting a strip of 0.125-inch steel to them.

Test jig.- The test jig was the one described in reference 1. The method of attaching the specimens to the jig was modified, however, in that the specimens were not bolted between the heavy loading bars of the jig. Instead, two steel strips 0.125-inch thick were bolted between the two sets of loading bars in such a manner that a 1-inch width of each strip was left exposed. The specimens overlapped these exposed widths of the steel strips and were riveted to them. The photograph of the test setup (fig. 2) shows these and other details.

Loading procedure.- Small loads were applied to the specimen and the jig was adjusted until the dial gages on the two sides of the specimen gave approximately equal readings. On most specimens two test runs were made, the first one to an arbitrarily selected load to check for the existence of permanent set, the second one to the load at which the specimen collapsed. Dial gage readings were taken at each increment of load until the rate of deformation became excessive.

TEST RESULTS

Check tests on solid webs.- The load-displacement curves obtained in the previous investigation had shown large irregularities that were attributed to play in the bolt holes (reference 1). The change from bolted attachment to riveted attachment was made partly to alleviate this difficulty. For the purpose of comparing the two methods of attachment, three webs without holes were tested. The dimensions of these webs and the test results are given in table 2. In agreement with the method of calculation used in reference 1, the effective length L_e of the specimens was taken as

$$L_e = L - \frac{h}{2}$$

for the computation of the collapsing stresses. The stresses designated calculated are based on the empirical curves for τ_{coll} given in figure 3. The ratios of experimental to calculated strength for the three check tests are higher than the average ratios developed in the tests of reference 1, but they are about equal to the highest ratios developed in those tests.

The load-displacement curves are shown in figure 4; they are free from the irregularities found in many of the tests of reference 1. The loads at which the curves depart from the straight line agree closely with the loads at which the first buckles were observed. The critical loads thus defined experimentally fall between the critical loads calculated by

L-323

standard formulas for flat plates with supported edges and with clamped edges, respectively. At loads below the critical, the observed displacements agree with the calculated displacements within the probable error of reading the dial gages.

Method of evaluating tests of perforated webs.- It will be assumed in the analysis of the test data that there is no ineffectiveness at the ends of the shear webs. This assumption probably represents the actual conditions in the test specimens fairly well, because all specimens had flanged ends. The assumption of no ineffectiveness is conservative; whereas any assumption of ineffective ends, such as was made in reference 1, may be unconservative. (Note that this statement applies only when allowable stresses are being derived from test results; in stress analysis, the opposite would be true.)

Load-displacement curves and shear-stiffness factors.- The load-displacement curves of all specimens with lightening holes are presented in figure 5. It may be noted that no irregularities appear in these curves; this fact tends to confirm the belief that the irregularities found in the tests of reference 1 were caused by play in the bolt holes.

The shear displacement of a perforated web may be calculated by the standard formula for shear displacement of a solid web if the actual thickness of the web is replaced by a reduced effective thickness. The reduction factor, or efficiency factor, designated by η, may be obtained experimentally. Because the load-displacement diagram deviates from the initial straight line at the critical load that causes buckling of the sheet between perforations, it is necessary to give separate factors for the initial stiffness at low loads and for the stiffnesses at high loads. In analogy with the elastic moduli, the stiffnesses at high loads may be defined by tangents to the load-displacement curve or by secants. Only the definition by secants will be used in this paper.

The experimental factors for initial shear stiffness, defined by the straight-line parts of the load-deformation diagrams, can be represented fairly well by empirical formula

$$\eta_o = \left(1 - \frac{D}{b}\right)\left[1 - \left(\frac{D}{h}\right)^3\right] \tag{1}$$

In figure 6 are shown the ratios of the experimental factors to the factors calculated by this formula. The majority of the test points fall within a ±15 percent scatter band, but there appears to be a slight decrease in the factor as the ratio h/t increases.

The initial shear stiffness is maintained until the critical load is reached; as the load passes the critical value and buckles form, the shear stiffness begins to decrease. Of practical interest in stress analysis is the shear stiffness at the design yield load. Experimental values were obtained from the load-deformation curves for an assumed design yield load equal to two-thirds the allowable load defined by equation (8), which appears later. Figure 7 indicates that a generally conservative estimate of the shear-stiffness factor at the design yield load, or at any other load P within the elastic range, may be obtained by the formula

$$\eta = \eta_o \frac{P_{cr}}{P} \left(P > P_{cr}\right) \qquad (2)$$

The critical loads used to establish the points on figure 7 were calculated by formula (3), given in the following section.

Attention is called to the narrow range of P/P_{cr} over which formula (2) has been verified; the formula should not be used too far beyond this range.

<u>Critical load</u>.- The critical load at which buckling begins between the perforations was determined by inspection and is indicated by a circle on each diagram of figure 5. It may be noted that the critical load determined in this manner agrees fairly well with the load at which the load-displacement diagram departs from the initial straight line. The critical load can be represented by the empirical formula

$$P_{cr} = Lt\left[\tau h_{cr}\left(1 - \frac{D}{h}\right) + \tau c_{cr} \frac{D}{h}\right] \frac{c'}{b} \qquad (3)$$

The critical load calculated by this formula is indicated on each diagram by a horizontal line. The calculated load is high for a number of specimens; but, because this discrepancy may be explained by lack of initial flatness and because the practical importance of the critical load is slight, no attempt was made to improve the formula.

L-323

Collapsing load.- The experimental collapsing loads are given in table 1. The analysis of the tests showed that a new formula was needed because the empirical formula for collapsing stress, developed in reference 1, becomes very unconservative for large values of h/t and of D/h. It was found that the stresses can be represented approximately by the formula

$$\tau_{coll} = \left[\tau_h \left(1 - \left(\frac{D}{h}\right)^2\right) + \tau_c \sqrt{\frac{D}{h}}\right] \frac{c'}{b} \tag{4}$$

The stress given by formula (4) is the stress on the gross section. The stress on the net section between holes is obtained by omitting the factor c'/b from the formula.

The ratios of the experimental stresses to the stresses calculated by formula (4) are plotted in figure 8 against the ratio h/t. The ratio of experimental to calculated stress apparently decreases somewhat as the ratio h/t increases; the decrease can probably be explained largely by the difficulty of producing flat specimens as the ratio h/t increases.

Figure 8 may be used to derive correction factors k for the shear stress τ_{coll} as indicated by the curves k_{av} and k_{all}. Curve k_{av} represents a correction factor intended to make formula (4) represent the average of the test data and is given by the equation

$$k_{av} = \left[1 - 3.5 \left(\frac{h}{1000t}\right)^2\right] \tag{5}$$

Curve k_{all} represents a correction factor intended to give a conservative allowable load for design purposes and is given by the equation

$$k_{all} = (0.85 - 0.0006\ h/t) \tag{6}$$

The equation

$$P_{av} = k_{av}\ Lt\tau_{coll} \tag{7}$$

gives an average value of the collapsing load, and the equation

$$P_{all} = k_{all} \, Lt\tau_{coll} \tag{8}$$

gives a conservative allowable value of the collapsing load.

Inspection of figure 8 shows that most test points fall within a ±15 percent scatter band about the curve representing k_{av}, with all distinct "misses" falling above the band. The stresses τ_h and τ_c in equation (4) are based on the empirical curves of figure 3. A study of the data on which figure 3 is based and of the check tests presented in table 2 indicates that the curves of figure 3 may be conservative by more than 30 percent. A scatter band of ±15 percent width indicates, therefore, that formula (7) represents the tests of perforated webs as well as the accuracy of the basic curves of figure 3 will permit.

Inspection during the last stages of the tests, after the dial gages had been removed, gave the impression that some specimens deformed much more than others before collapsing. This observation indicates that the termination of the useful life of a specimen might be defined better by the load-displacement curve than by the collapse of the specimen. A tentative application of this method was made by defining the useful ultimate load by the intersection of the load-displacement curve with a secant from the origin having a slope equal to one-third the slope of the initial tangent. The value "one-third" was chosen to make the definition applicable to all tests. The slope used was determined by the specimen with the smallest deformation. The loads defined by the secants average about 9 percent lower than the collapsing loads. The interesting point, however, is the scatter from the mean of the ratios of the experimental loads to the loads calculated by formula (7). When the collapsing loads were used, the average deviation from the mean was 0.12; when the loads determined by the secants were used, the average deviation from the mean was only 0.07, in spite of the fact that some of the load-displacement curves had to be extrapolated.

Revised analysis of previous strength tests.- The tests on webs with flanged holes described in reference 1 were reanalyzed for comparison with the new formulas. The results of the analysis are plotted in figure 9 and show that, for specimens with reamed holes, formula (5) represents the average fairly well, and formula (6) gives conservative values for design. Of the specimens with drilled holes, a few fall below the design curve, which suggests that the allowable loads given by formula (8) should be reduced somewhat when the web is attached by bolts that may develop play.

Design charts.- In order to facilitate the application of the formula for allowable load, a set of design charts is presented in figure 10. The charts are based on formula (8), but for convenience the running shear load $S/h = P_{all}/L$ is plotted rather than the shear load itself.

If the depth, the thickness, and the hole diameter of a web are held fixed while the hole spacing is being varied, one certain hole spacing will be found to give a maximum strength-weight ratio of the web (reference 1). Figure 11 is a design chart, based on the assumption that the optimum hole spacing is used. The lines of constant weight drawn on this chart are almost horizontal, which indicates that the strength-weight ratio is nearly independent of the hole size for a web of given depth and given strength. Over a limited region, the lines of constant weight have a definite upward slope at large values of D/h, which indicates that the strength-weight ratio is improved somewhat if the largest possible hole is used. This gain should be balanced against the accompanying loss in shear stiffness.

Permanent set.- Checks for permanent set were made on 15 specimens, as listed in table 1. In order to be of maximum value, these checks should have been made at loads corresponding to the design yield loads, that is, at $0.67P_{all}$ or slightly higher, depending on the design requirements chosen. It was not possible to predict P_{all} at the time the tests were being made, and it was desired to avoid damage to the specimens by the set tests. The loads chosen for the set tests, therefore, were in general lower than $0.67P_{all}$; as table 1 shows, however, only two tests out of 15 were more than 20 percent below $0.67P_{all}$, and six tests were above this value. No permanent set was found in any specimen, a fact tending to confirm the view that the permanent set in the specimens of reference 1 was caused largely by slip in the bolted joints. A study of the avialable evidence indicates that the shear stress in the net section between perforations may be a practical criterion for estimating the permanent set, but the evidence is insufficient to allow quantitative conclusions.

DISCUSSION OF FORMULAS

The tests presented in this paper, together with the tests of reference 1, cover a range of parameters approximately as follows:

$$0.15 < D/h < 0.75$$

$$2 < b/D < 2.6 \text{ for } D/h \approx 0.15 \text{ and } 1.5 < b/D < 2.6 \text{ for } D/h > 0.3$$

$$45 < h/t < 300$$

$$0.14 < c/h < 1.4$$

The formulas given for the stiffness and the strengh of perforated webs should be applicable in this range. The coverage is much less complete in the range of the new tests ($0.5 < D/h < 0.75$; $150 < h/t < 300$); some caution should therefore be used in this range.

A study of formula (4) when the parameters approach limiting values indicates that the formula probably becomes conservative in two limiting cases; webs with large holes spaced far apart, and webs with small holes closely spaced. The second case may be dismissed as of small practical interest, but the first case is of some use. Formula (4) gives for this case ($D/h \to 1$; $c >> h$)

$$\tau_{coll} = \tau_c \frac{c'}{b}$$

The correct value evidently is

$$\tau_{coll} = \tau_h \frac{c'}{b}$$

provided that ineffectiveness at the ends of each segment is neglected, an assumption that may be interpreted as requiring roughly $c > 10h$. Specimen 5 with $c/h \approx 1.4$ gave close agreement between experimental and calculated strength. Consequently, the conservativeness of formula (4) indicated by consideration of the limiting case $c >> h$ should not be expected to exist until the ratio c/h is far above 1.4.

It should be remembered that the test webs were attached to flanges of very great stiffness. Actual webs may be

L-323

attached to flanges of low stiffness and strength and special consideration must be given to this factor when necessary, particularly when the ratio D/h is large. When the holes are large, it may become necessary to rely on the attachment flanges to carry part of the shear across the region of the hole; the strength and stiffness of the structure will then depend not only on the properties of the web but also on the properties of the attachment flanges.

CONCLUSIONS

The most important conclusions drawn from the analysis of the tests on shear webs with flanged, round lightening holes are as follows:

1. The strengths of the webs may be related to the strengths of solid unstiffened webs by a simple empirical formula. The accuracy of the strength prediction is about equal to the accuracy of the strength prediction for solid unstiffened webs, which is based on empirical curves.

2. The shear stiffnesses of the webs may be predicted by simple empirical formulas with about the same degree of accuracy as the strengths.

3. Shear webs designed for a given ultimate load by the proposed design formula will probably show no permanent set at the design yield load unless the shear stress over the net section between holes is about equal to the yield stress.

Attention is directed to the fact that the results apply directly only when the flanges to which the webs are attached are not highly stressed by the shear force in the web. Special consideration must be given to webs with large holes and weak attachment flanges.

Langley Memorial Aeronautical Laboratory,
National Advisory Committee for Aeronautics,
Langley Field, Va.,

REFERENCE

1. Kuhn, Paul: The Strength and Stiffness of Shear Webs with and without Lightening Holes. NACA A.R.R., June 1942.

TABLE 1

PERFORATED SHEAR WEBS

Dimensions of specimens							
Specimen (a)	L (in.)	t (in.)	h (in.)	D (in.)	b (in.)	c (in.)	c' (in.)
1	30.63	0.0202	4.02	2.63	4.38	1.75	1.38
2	33.25	.0320	4.02	2.63	4.75	2.12	1.75
4	40.25	.0526	4.06	2.63	5.75	3.12	2.75
5	57.75	.0614	4.05	2.63	8.25	5.62	5.31
6	40.25	.0200	5.00	3.50	5.75	2.25	1.75
7	42.00	.0324	5.02	3.50	6.00	2.50	2.00
8	42.88	.0426	5.08	3.50	6.13	2.63	2.13
9	45.50	.0527	5.00	3.50	6.50	3.00	2.50
10	52.50	.0619	5.02	3.50	7.50	4.00	3.50
11	49.00	.0200	6.02	4.50	7.00	2.50	2.00
12	49.00	.0327	6.02	4.50	7.00	2.50	2.00
13	52.50	.0406	6.00	4.50	7.50	3.00	2.50
14	54.25	.0510	6.05	4.50	7.75	3.25	2.75
15	57.75	.0611	6.05	4.50	8.25	3.75	3.25
16	54.25	.0326	10.05	4.50	7.75	3.25	2.75
17	54.25	.0383	10.00	4.50	7.75	3.25	2.75
18	56.00	.0539	10.03	4.50	8.00	3.50	3.00
19	56.00	.0613	10.06	4.50	8.00	3.50	3.00

Test results									
Specimen (a)	Exp. P_{coll} (kips)	Calc. P_{av} (kips)	$\frac{\text{Exp.}}{\text{Calc.}}$	P_{all} (kips)	P_s (kips)	$\frac{P_s}{0.67 P_{all}}$	η_0	η (at $P = 0.67 P_{all}$)	Exp. τ(net) (kips/sq in.)
1	2.44	2.58	0.94	2.19	—	—	0.288	0.214	12.56
2	6.43	7.38	.87	6.07	—	—	.322	.304	16.42
4	20.70	24.85	.83	20.38	12.80	0.94	.396	.363	20.46
5	46.40	47.05	.99	38.69	18.40	.71	.496	.572	20.32
6	2.31	2.38	.97	2.12	1.30	.92	.257	.149	9.44
7	6.28	7.07	.89	5.82	5.00	1.29	.275	.217	13.86
8	15.10	12.83	1.18	10.48	4.75	.68	.289	.257	23.82
9	21.60	21.18	1.02	17.31	9.40	.81	.304	.295	23.40
10	28.00	34.06	.82	27.89	16.70	.90	.352	.351	18.45
11	2.23	2.15	1.03	2.10	1.70	1.21	.207	.112	7.94
12	5.53	6.68	.83	5.59	4.25	1.14	.207	.157	12.07
13	14.40	11.53	1.25	9.49	5.25	.83	.231	.220	20.29
14	20.70	19.20	1.08	15.69	10.00	.96	.246	.299	21.08
15	23.65	29.66	.80	24.20	15.30	.95	.268	.331	17.01
16	5.40	4.84	1.12	4.80	3.50	1.09	.381	.200	8.60
17	13.15	7.37	1.79	6.68	6.50	1.46	.381	.265	17.83
18	22.30	17.03	1.31	14.28	—	—	.397	.303	19.70
19	24.40	22.42	1.09	18.58	13.50	1.09	.398	.318	18.95

[a] Specimen 3 not tested.

TABLE 2

SOLID SHEAR WEBS

Specimen	L_e (in.)	t (in.)	h (in.)	P_{coll} (kips)	Exp. τ (kips/sq in.)	Calc. τ (kips/sq in.)	$\frac{\text{Exp.}}{\text{Calc.}}$
21	63.56	0.0343	5.00	26.90	12.33	8.33	1.48
22	63.13	.0351	6.00	20.80	9.40	7.08	1.33
23	61.06	.0344	10.00	11.30	5.38	4.14	1.30

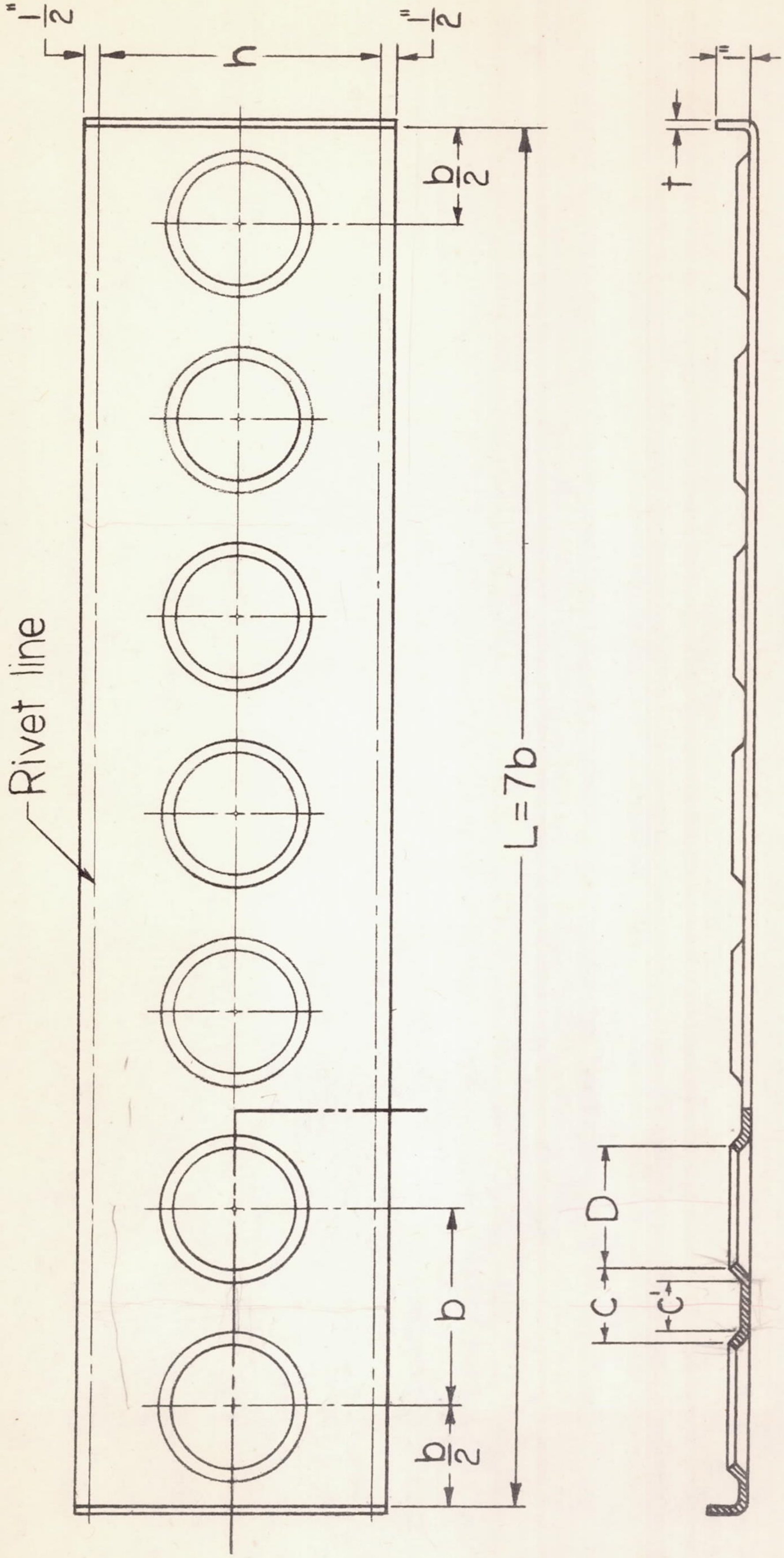

Figure 1.- Standard test specimen.

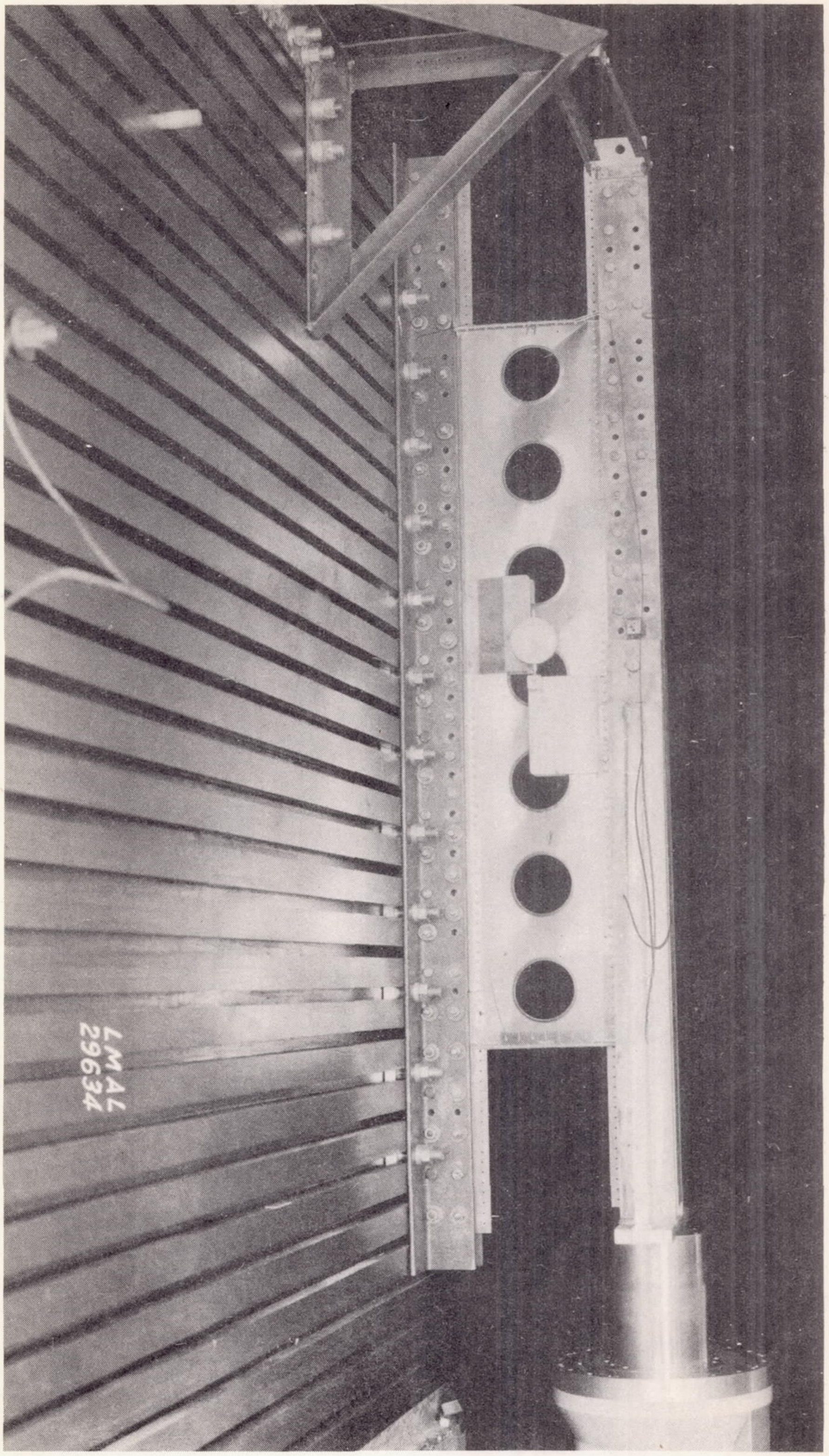

Figure 2.- Test jig in operation.

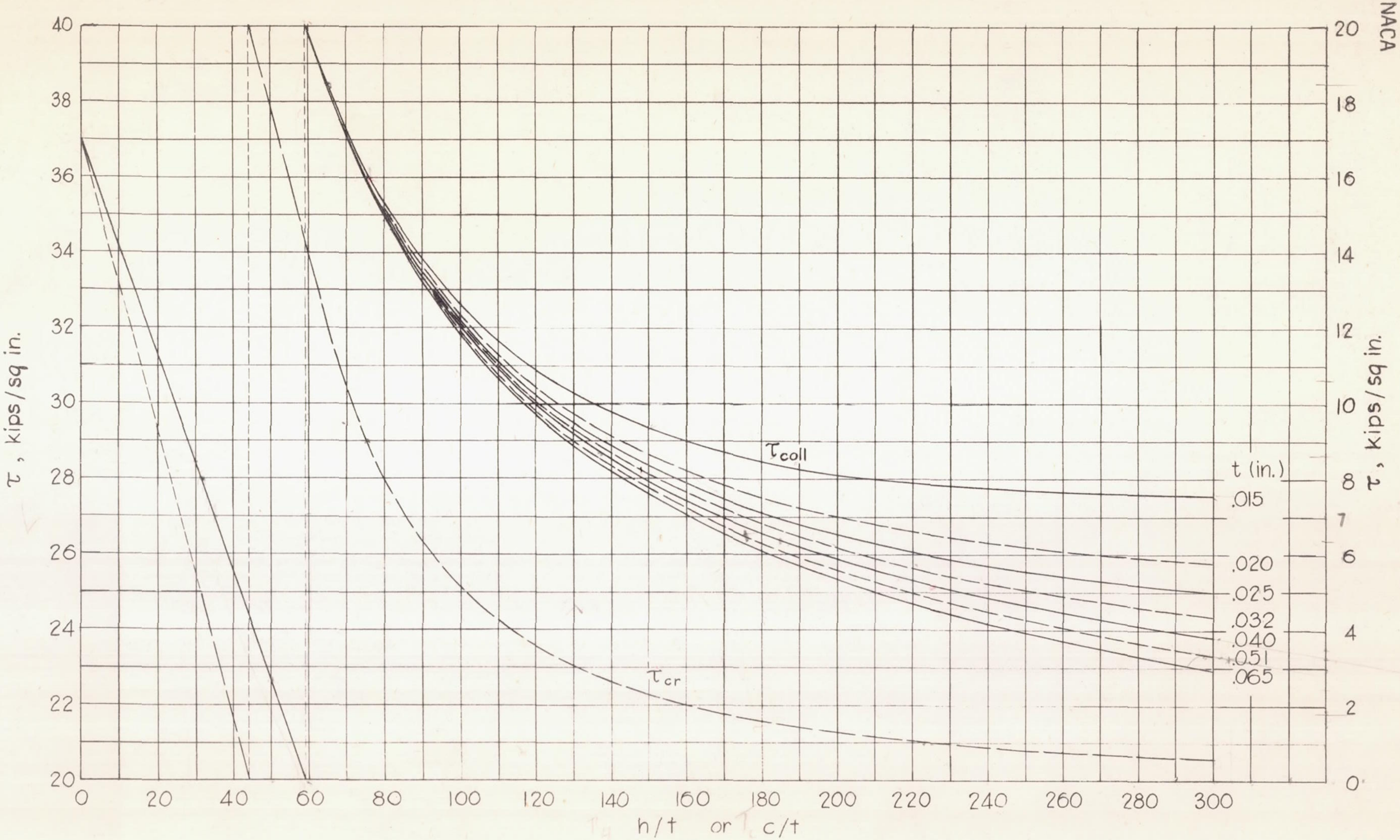

Figure 3.- Critical and collapsing shear stresses for solid webs of 24S-T aluminum alloy. From reference 1.

(Measure with 40ths scale)

Fig. 3

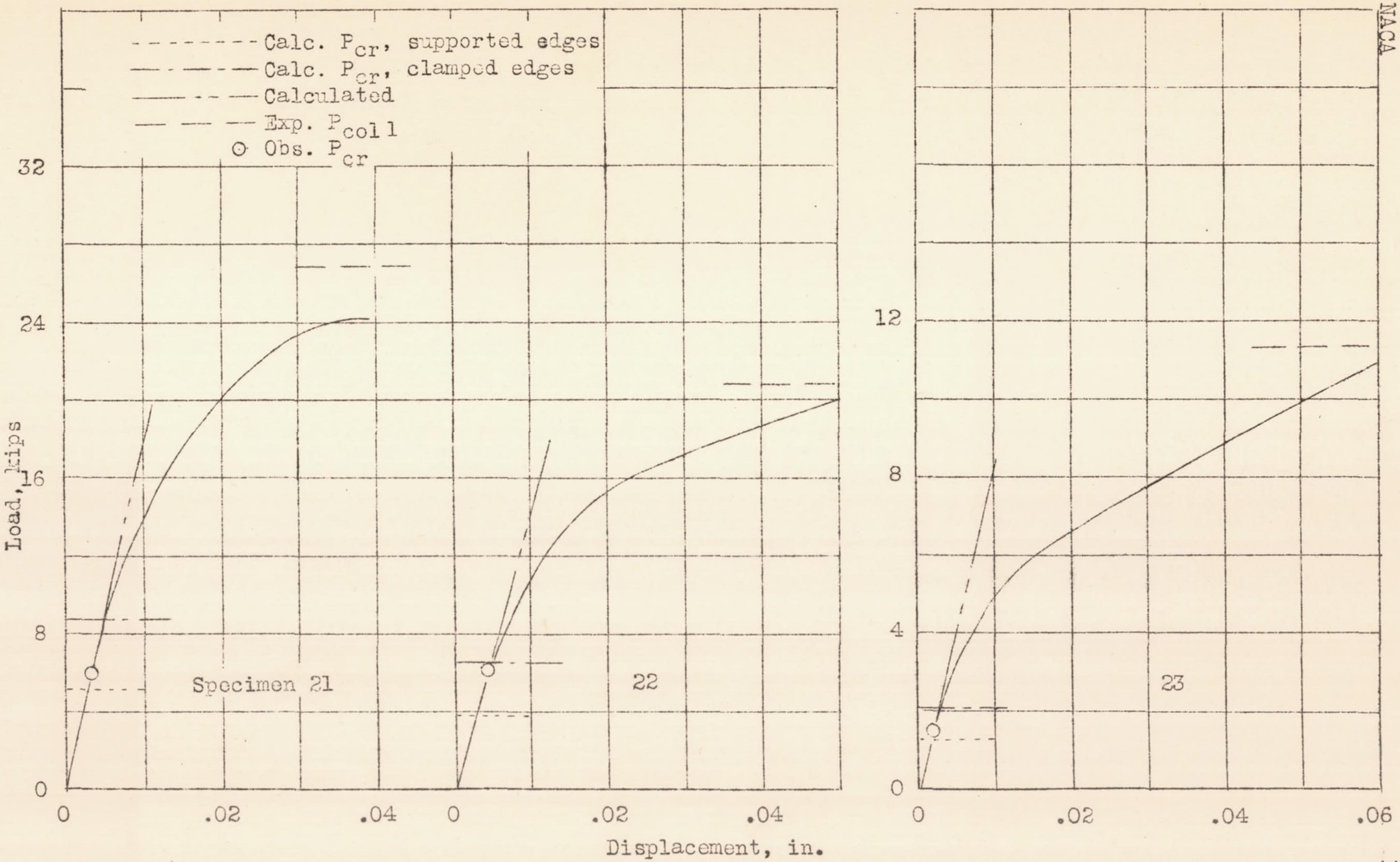

Figure 4.- Load-displacement curves for solid webs.

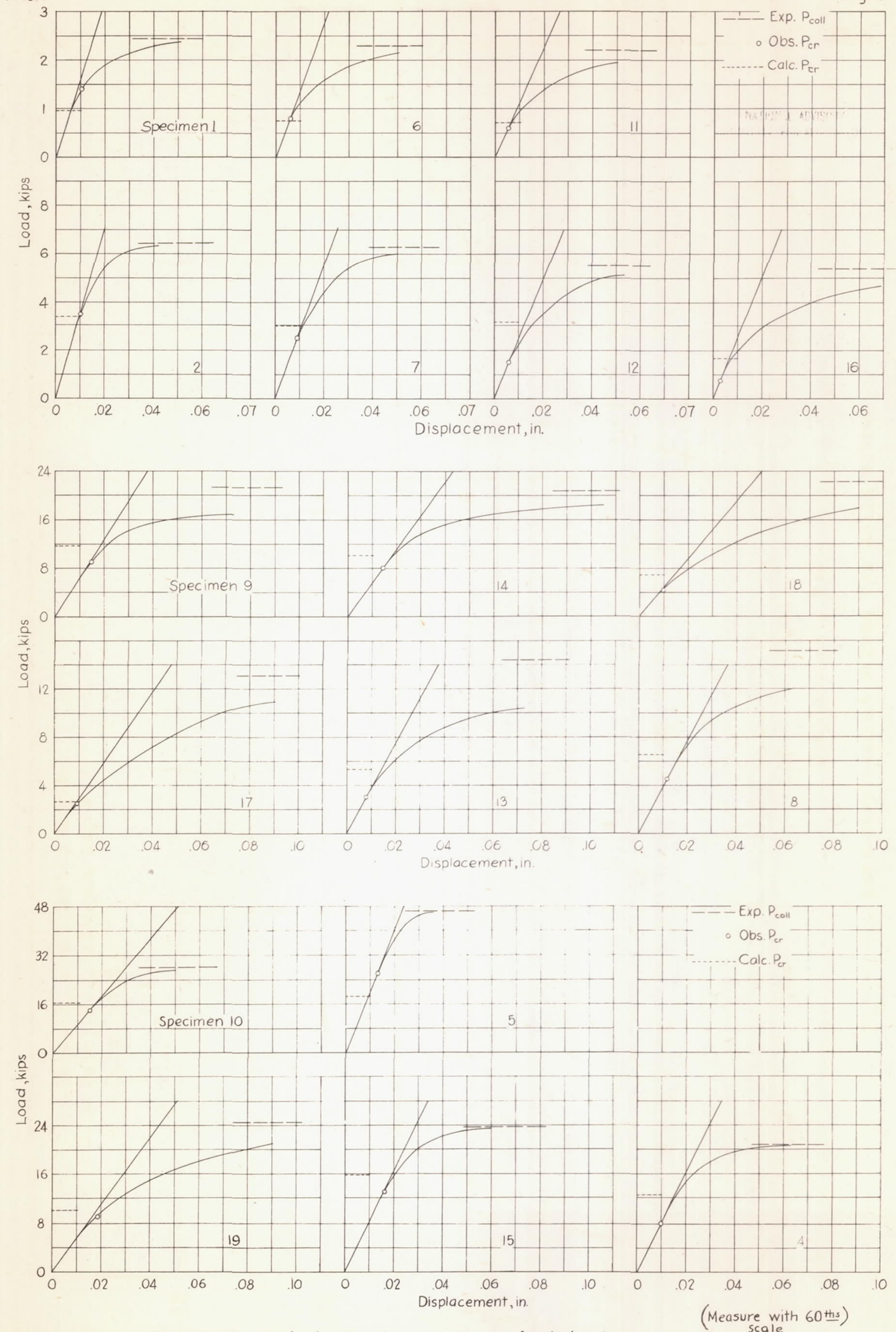

Figure 5.- Load-displacement curves for perforated webs.

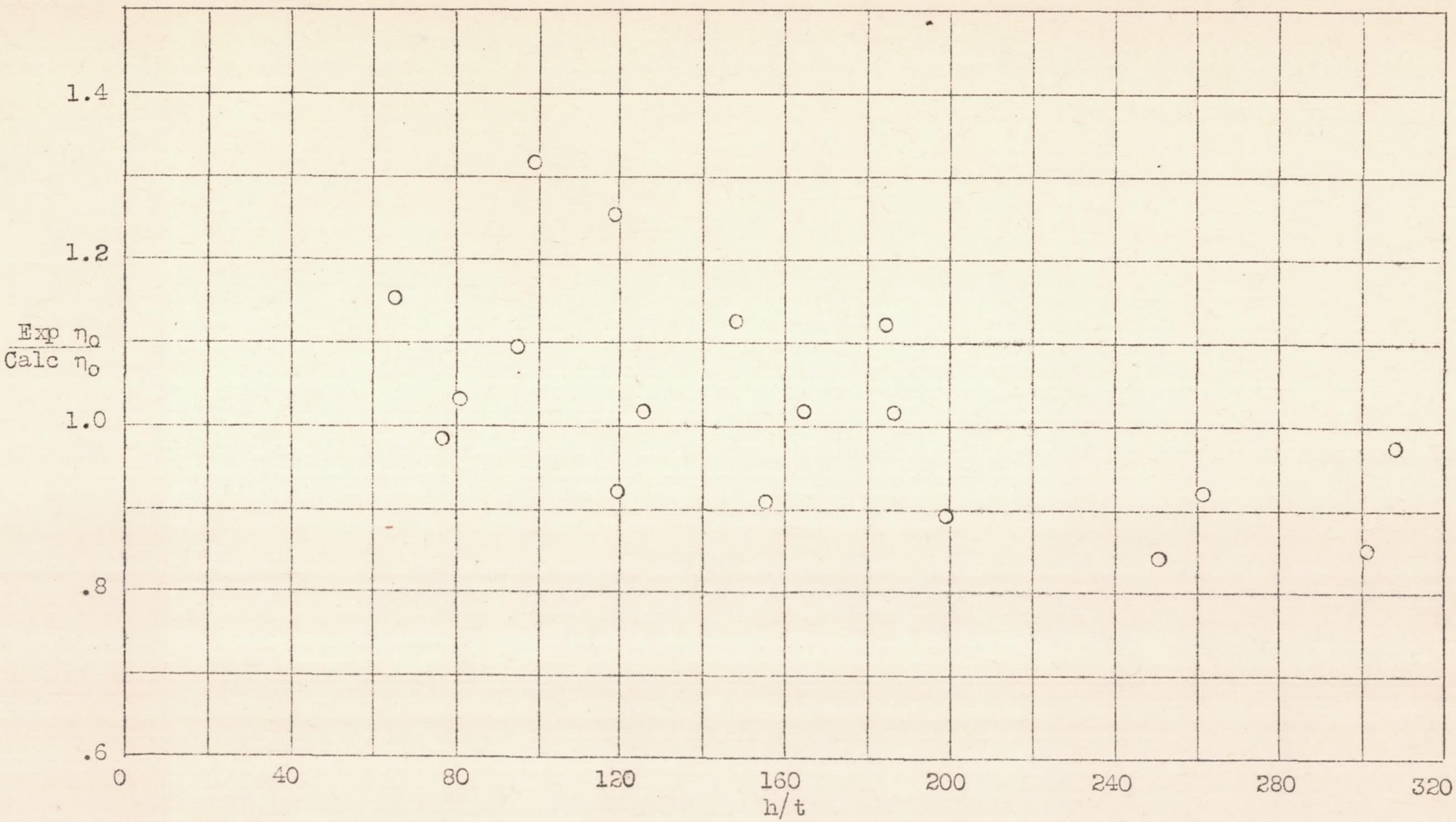

Figure 6.- Ratios of experimental to calculated factors of initial shear stiffness.

L-323

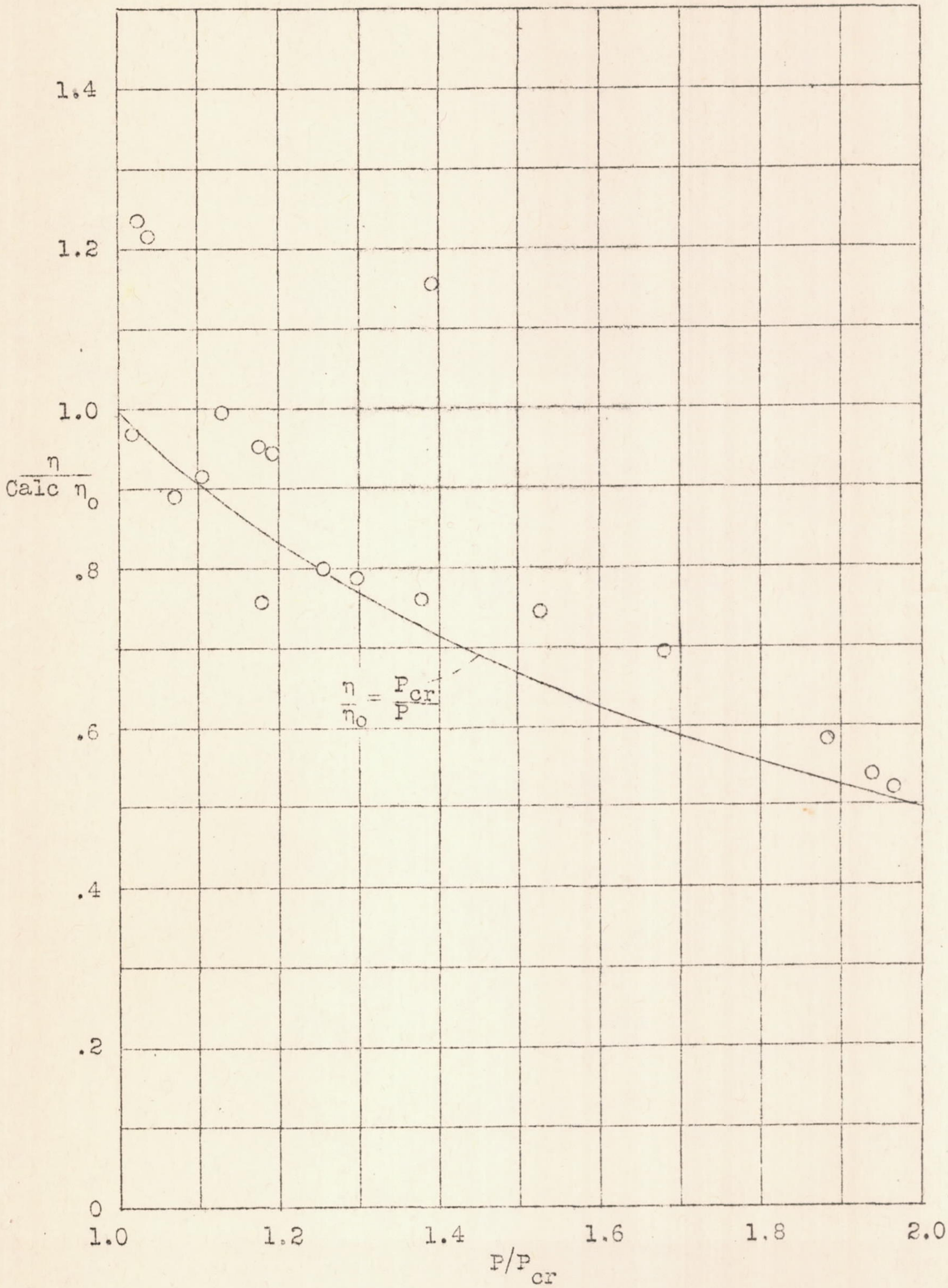

Figure 7.- Decrease of shear-stiffness factor with loading ratio. Points taken for $P = 0.67\ P_{all}$.

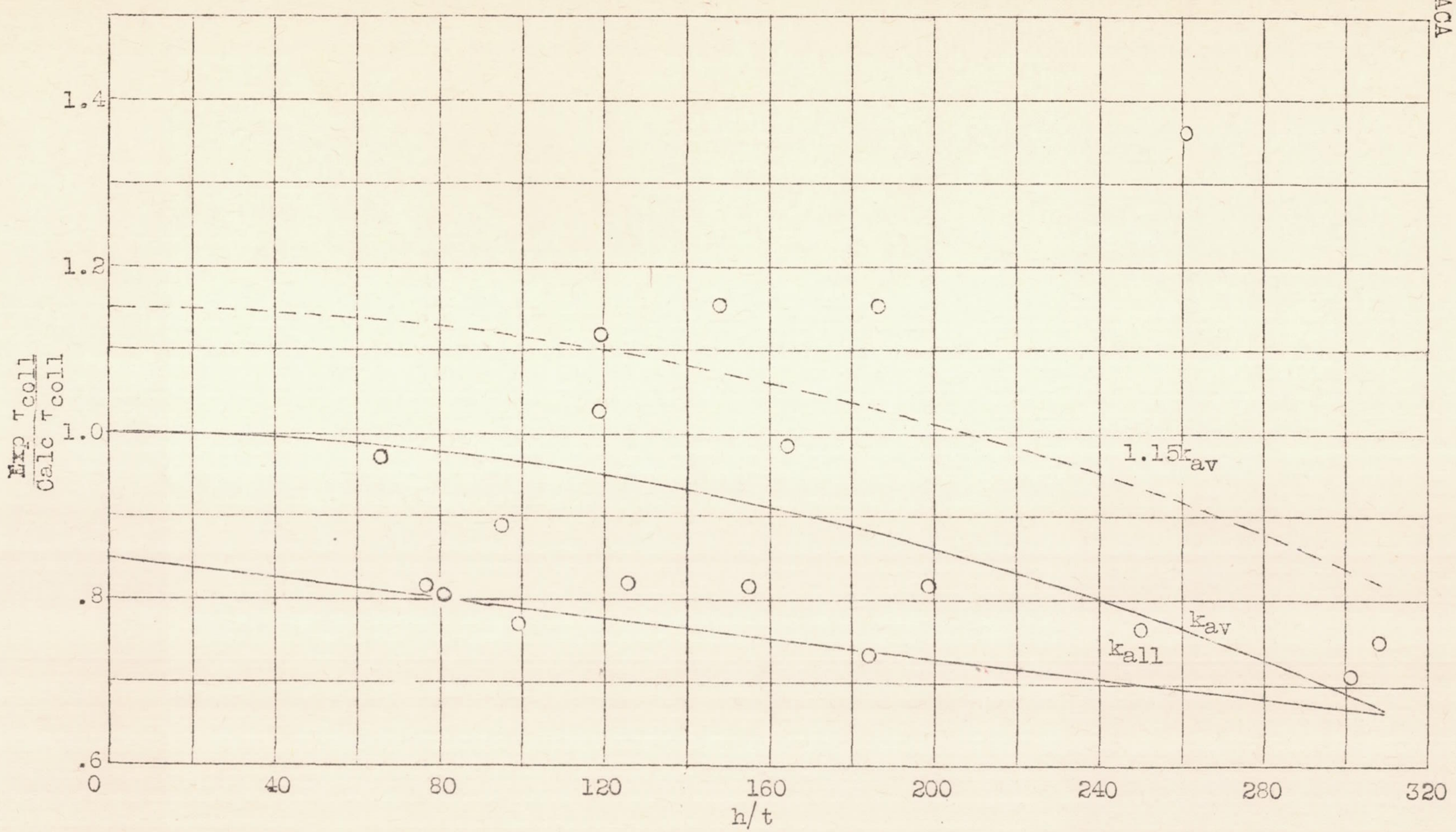

Figure 8.- Ratios of experimental to calculated collapsing stresses. Calculated stresses are based on formula (4).

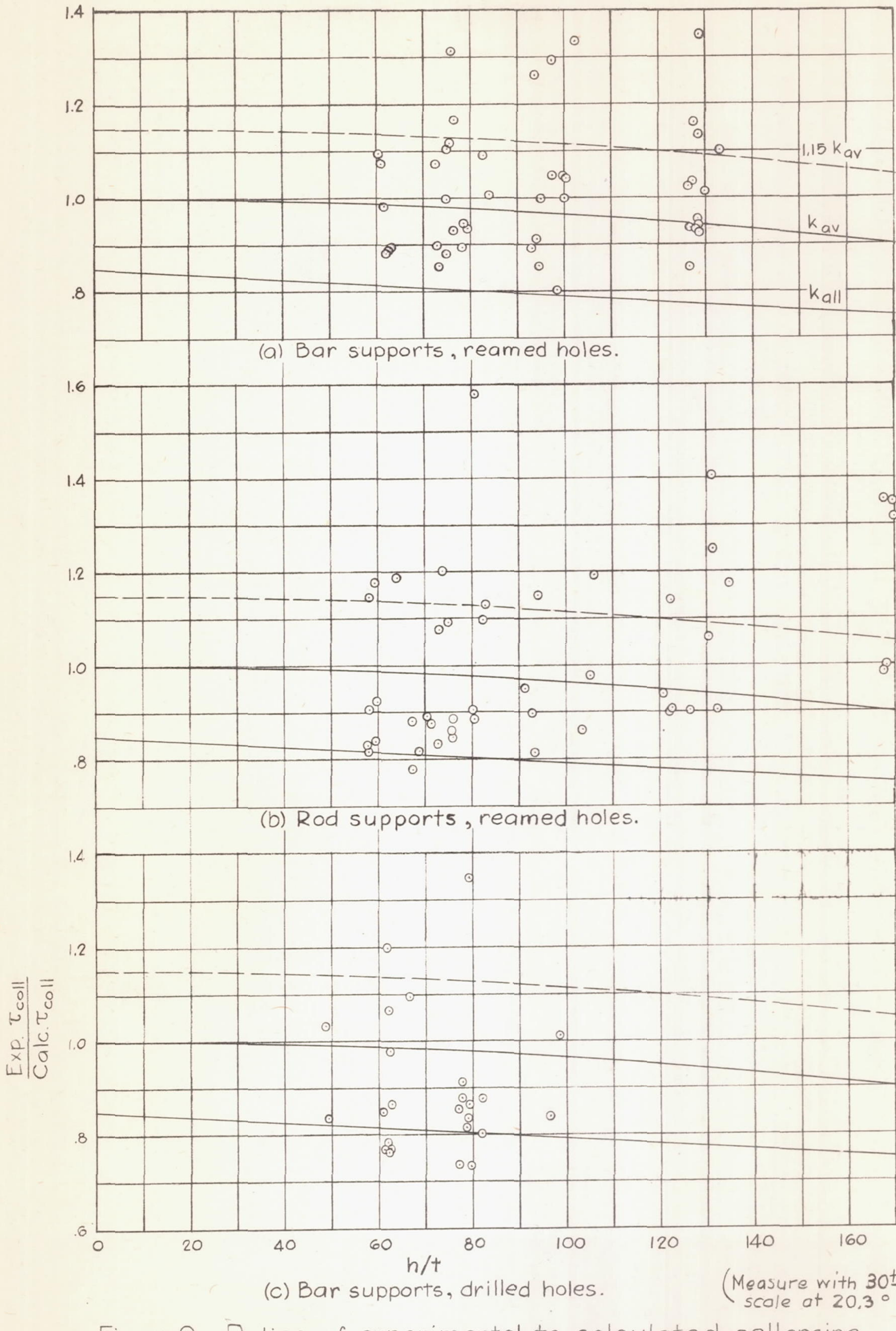

(Measure with 30ths scale at 20.3°)

Figure 9.- Ratios of experimental to calculated collapsing stresses for tests of reference 1. Calculated stresses are based on formula (4).

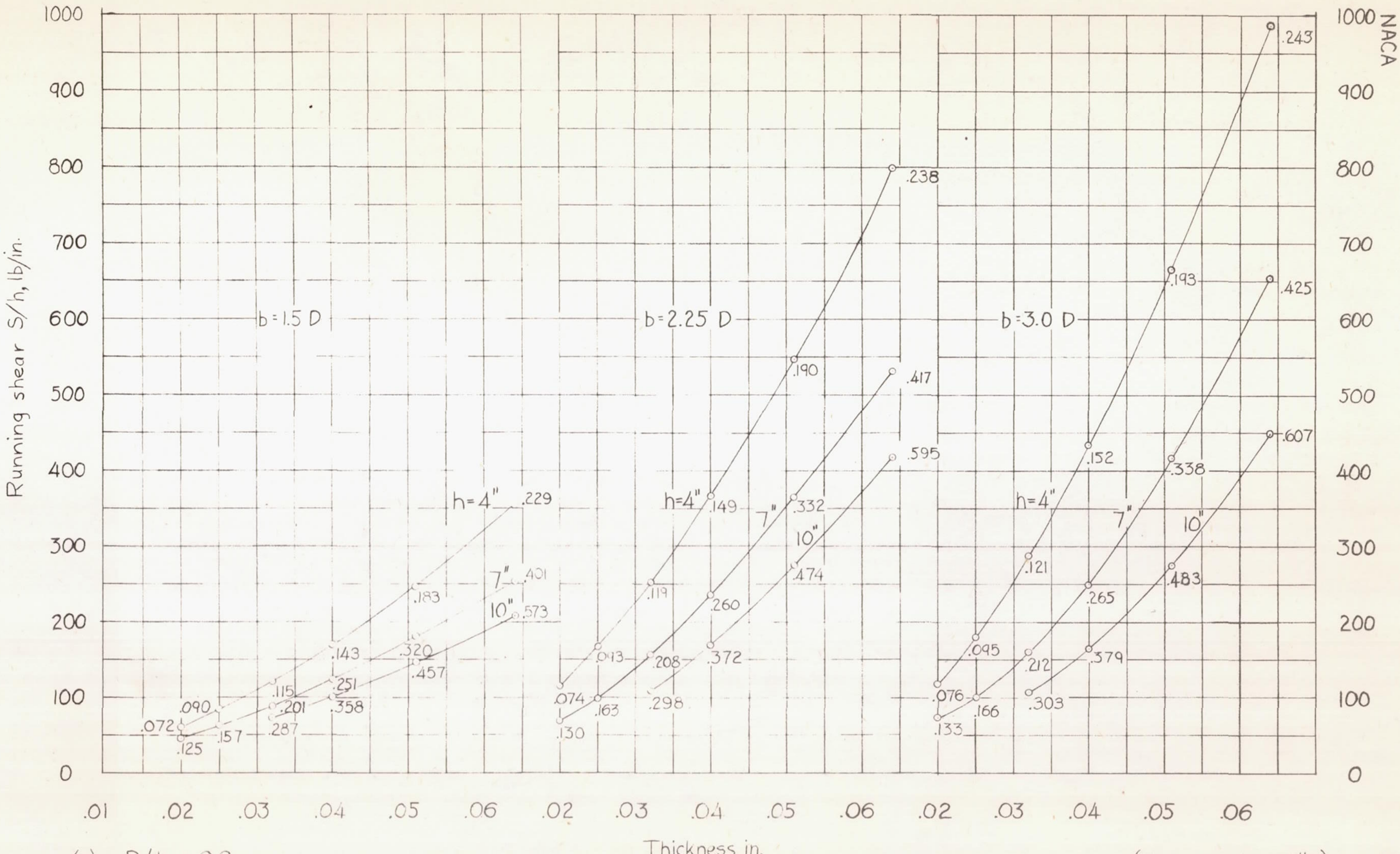

(a) D/h = 0.2.

Figure 10.– Design chart for webs with round lightening holes having 45° flanges. Material 24 S-T aluminum alloy. Numbers near circles give running volume of material, $in.^3/in.$

NACA

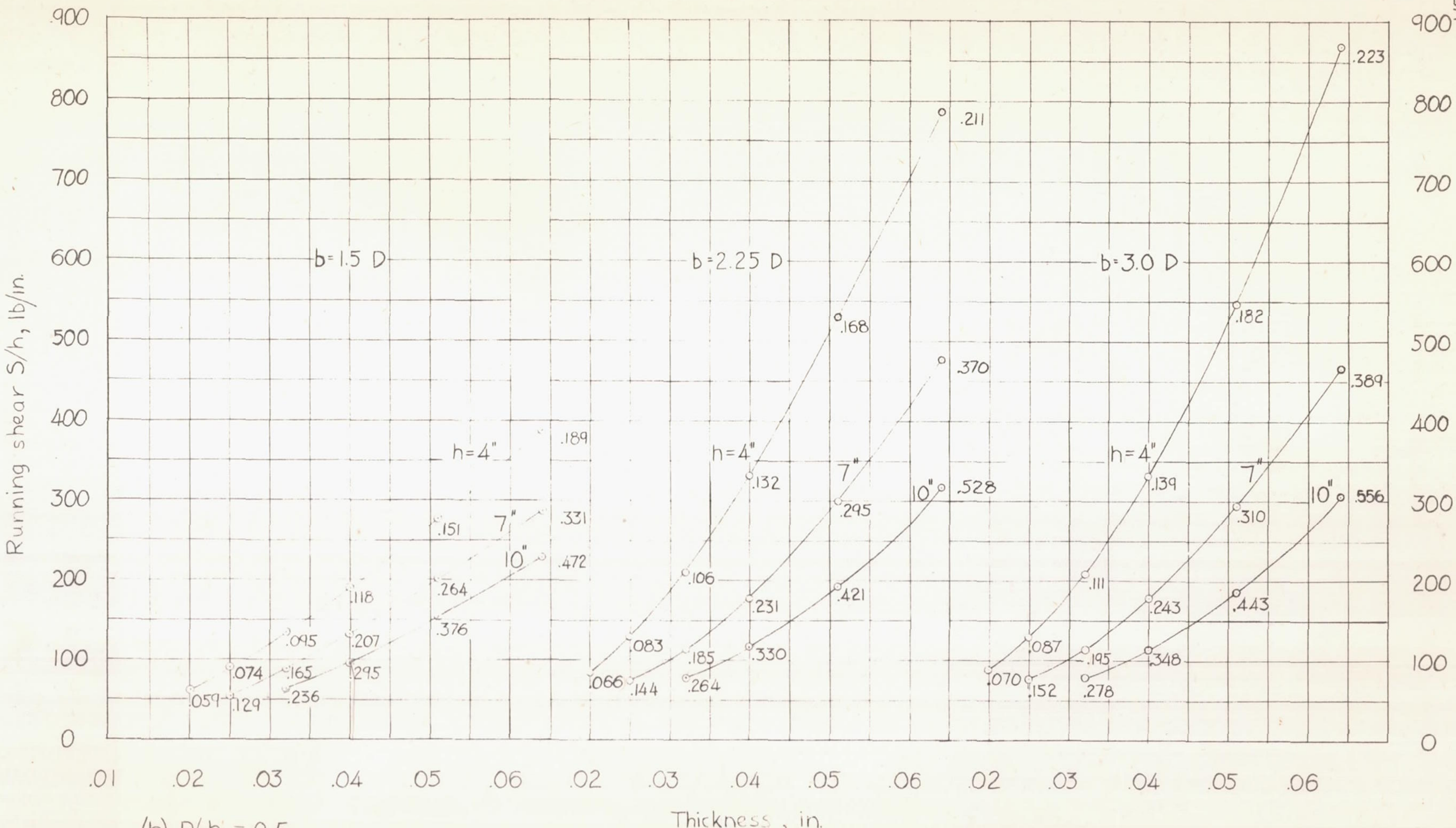

(b) D/h = 0.5.

Figure 10.- Continued.

(Measure with 40ths scale)

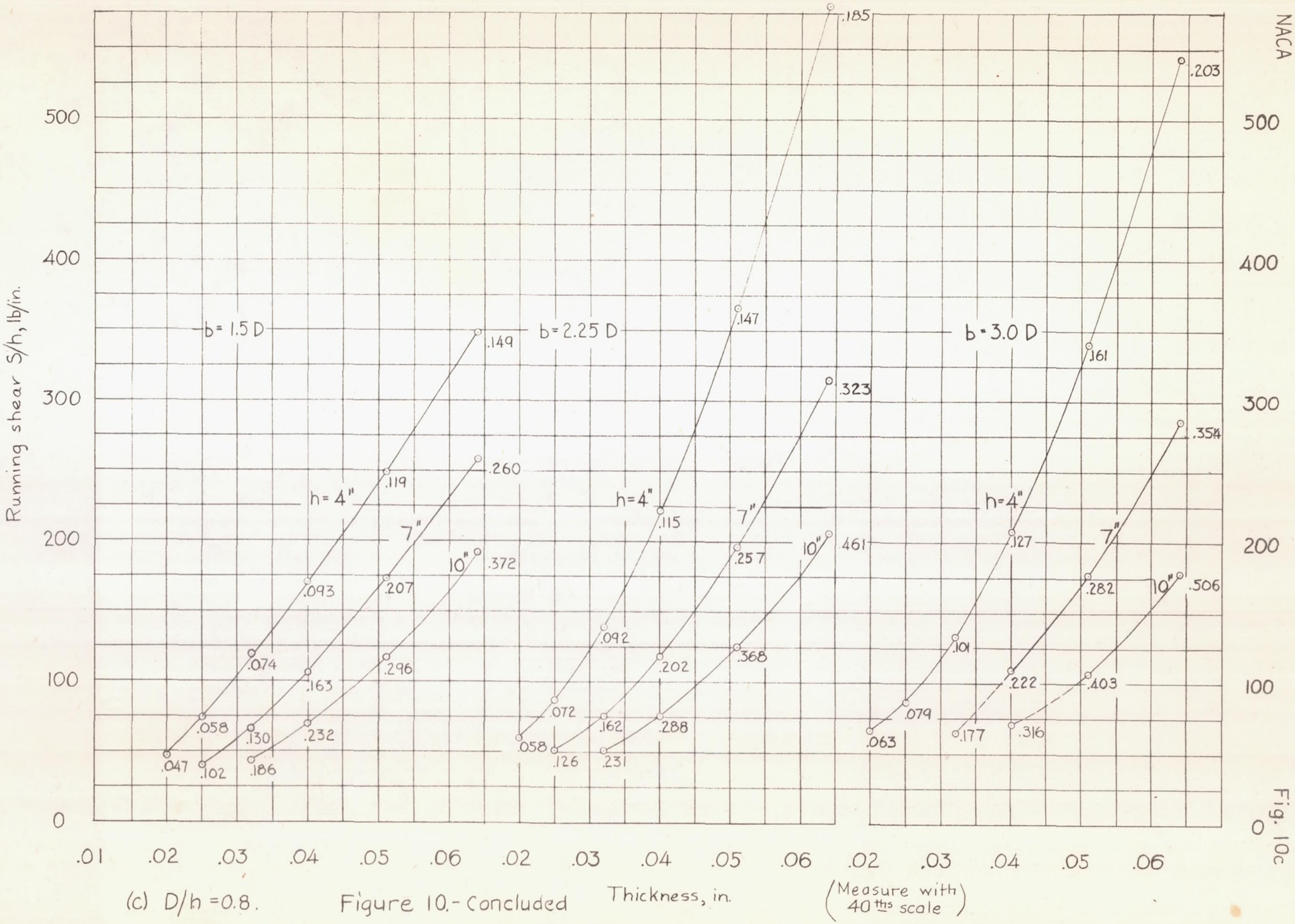

(c) D/h = 0.8.

Figure 10.- Concluded

Fig. 10c

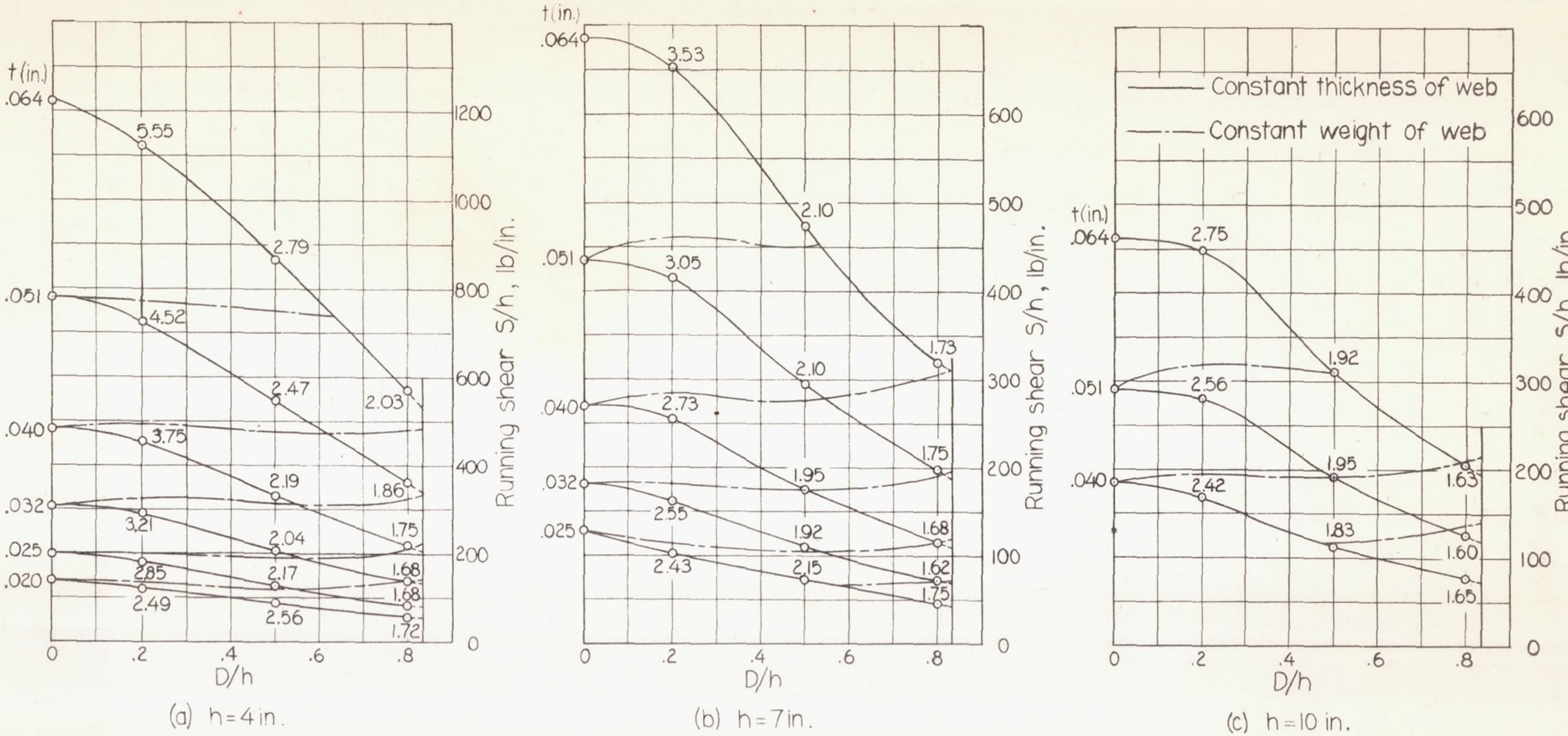

Figure 11 – Design chart for webs with round lightening holes having 45° flanges and using optimum hole spacing.

Material 24S-T aluminum alloy. Numbers near circles give optimum values of b/D.

Example: The optimum design for a web 7 inches deep to carry S/h = 320 pounds per inch run would be 0.064 inch thick with a D/h of 0.8 and would equal in weight a solid web 0.041 inch thick.

(Measure with 40ths scale)